Volume 4
Number 6
June 2025
Pages 811–982

Environmental Science Advances

rsc.li/esadvances

ISSN 2754-7000

ROYAL SOCIETY OF CHEMISTRY

PAPER

Ryota Nakajima *et al.*

Development of a novel semi-automated analytical system of microplastics using reflectance-FTIR spectrometry: designed for the analysis of large microplastics

Environmental Science Advances

ROYAL SOCIETY OF CHEMISTRY

PAPER

View Article Online
View Journal | View Issue

Check for updates

Cite this: *Environ. Sci.: Adv.*, 2025, **4**, 901

Development of a novel semi-automated analytical system of microplastics using reflectance-FTIR spectrometry: designed for the analysis of large microplastics†

Ryota Nakajima, *[a] Hiromi Sawada,[b] Shinichiro Hayashi,[b] Akishi Nara[b] and Mitsunari Hattori[b]

The (semi-) automation of microplastic analysis would dramatically accelerate the otherwise time-consuming and labor-intensive process, enabling more efficient identification of global microplastic distribution. Numerous methods have been proposed for the automated analysis of small microplastics (approximately less than 100 μm) on filters using micro-FTIR (Fourier Transform Infrared Spectroscopy). However, the development of automated analysis technology for relatively larger microplastics (*e.g.*, >500 μm), which can be handled with forceps, has progressed relatively slowly. In this study, we developed a device that enables semi-automated analysis of such large microplastics. This device modifies the reflection measurement accessory of FTIR for microplastic analysis and integrates it with an image recognition camera and a motorized stage. This system allows for the final output of the number, size, and polymer type of microplastics placed on a sample plate into a Microsoft Excel file in a single procedure. The accuracy rate of identifying degraded microplastics (comprising eight types of polymers) collected from environmental sources, including the ocean, using this device was over 98% when compared to the commonly used ATR (Attenuated Total Reflection)-FTIR method. Furthermore, the time required for analysis—from the placement of the sample and size measurement to material identification—was, on average, 6.6 times faster than conventional methods. The current MARS system can reliably and automatically identify environmentally degraded microplastics with a minimum size threshold of 400 μm, and it offers significant advantages in terms of reduced data collection time and high throughput for the processing of large microplastics.

Received 27th November 2024
Accepted 8th February 2025

DOI: 10.1039/d4va00400k

rsc.li/esadvances

Open Access Article. Published on 10 February 2025. Downloaded on 5/28/2026 11:32:46 AM. This article is licensed under a Creative Commons Attribution 3.0 Unported Licence.

Environmental significance

Microplastic analysis is time-consuming and labor-intensive, requiring manual handling and lengthy procedures for identifying quantity, size, and polymer types. Efficient microplastic analysis is crucial for monitoring environmental impacts, predicting trends, and evaluating mitigation measures. Microplastics pose threats to ecosystems and health, carrying toxic pollutants and disrupting organisms' biological systems. The study developed a semi-automated device using reflectance-FTIR spectroscopy integrated for large microplastics, achieving 98% accuracy and reducing analysis time by 6.6 times compared to a conventional method. This advancement addresses the inefficiencies in microplastic analysis, enabling faster and more reliable data collection critical for environmental monitoring and policy-making.

Introduction

The leakage of plastic debris into the natural environment is a global concern.[1] Specifically, microplastics, defined as water-insoluble synthetic polymers ranging from 1 μm to 5 mm in size, are particularly concerning pollutants, especially in aquatic ecosystems where they pose significant threats to the organisms living there.[2] These particles, categorized as either primary (manufactured to be less than 5 mm such as pellets and microbeads) or secondary (resulting from the degradation of larger plastics), can obstruct the digestive systems of organisms, potentially causing starvation and death.[3] Furthermore, microplastics can carry harmful pollutants like persistent organic pollutants (POPs) including polybrominated diphenyl ethers (PBDEs), benzotriazole UV-absorber and polychlorinated biphenyls (PCBs), leading to toxic exposure and endocrine disruption.[4] Continued monitoring of microplastics in the

[a]*Japan Agency for Marine-Earth Science and Technology (JAMSTEC), 2-15 Natsushima, Yokosuka, Kanagawa 237-0061, Japan. E-mail: nakajimar@jamstec.go.jp*

[b]*Thermo Fisher Scientific K.K., 3-9 Moriya, Yokohama, Kanagawa 221-0022, Japan*

† Electronic supplementary information (ESI) available. See DOI: https://doi.org/10.1039/d4va00400k

© 2025 The Author(s). Published by the Royal Society of Chemistry

Open Access Article. Published on 10 February 2025. Downloaded on 5/28/2026 11:32:46 AM. This article is licensed under a Creative Commons Attribution 3.0 Unported Licence.

environment is necessary for predicting future trends, and assessing the effectiveness of mitigation measures globally.[5]

One of the biggest obstacles in microplastic study is the effort and time required for the analysis. In case of microplastics that can be collected with standard manta/neuston nets from the surface water in aquatic environments, it is not uncommon for it to take several days to over 10 days to determine the quantity, polymer type, and size of microplastics from a single sample.[6] These three items are acknowledged as essential factors to understand the fate and impact of microplastics.[7] However, the effort, time, and human labor required to obtain these factors make rapid assessment of microplastics significantly challenging. In evaluating existing microplastic analysis procedures, we identified the need for a (semi-) automated instrument that allows rapid and efficient analysis of microplastics to determine their quantity, size, and polymer type.

Chemical analyses of microplastics to determine their polymer types are among the most labor-intensive and time-consuming processes. These chemical analyses include spectroscopy methods such as Fourier Transform Infrared Spectroscopy (FTIR) and Raman, as well as pyrolysis, with FTIR probably being the most widely used method.[8–12] For FTIR analysis, either FTIR with a single-reflection diamond Attenuated Total Reflection (ATR) or micro-FTIR is commonly used, depending mainly on particle size.[13] Generally, ATR-FTIR is employed for the analysis of microplastics that can be recognized with the naked eye and picked up with forceps or a sampling needle, with the suitable size of analyzed particles being larger than 500 μm,[14–16] and the technically lowest size limit being around 100 μm.[17] Micro-FTIR is generally used for smaller particles.[18] In this study, we focus on larger microplastics (>500 μm–5 mm)[17] that can be feasibly analyzed using ATR-FTIR.

In the ATR method, the sample particle is pressed against the prism to ensure close contact for analysis, making it well-suited for analyzing thick or irregularly shaped samples.[7,19] Yet, it takes a long time to analyze a large number of particles because each microplastic-like particle must be manually placed onto the ATR prism one by one and measured.[13] Since ATR analysis involves pressing the particle against the prism, it frequently destroys deteriorated microplastics due to the applied pressure. For this reason, the measurement of the size of all microplastic-like particles is carried out 'before' ATR analysis, resulting in measuring the size of particles that are not actually plastic, which again leads to a loss of time.

Reflectance-FTIR spectroscopy can be a solution to these problems, as it is a non-contact method that is non-destructive and allows high throughput of samples.[20] Reflectance-FTIR spectroscopy is commonly used in micro-FTIR for analyzing small microplastics on a metal mesh filter, but is generally not used for larger microplastic analysis, simply because they are too big to be measured by micro-FTIR. To date, in conventional FTIR (not micro-FTIR), there has not been a device available that uses the reflectance method to measure microplastics. By combining reflectance-FTIR with a motorized stage and an image capturing camera, it would be possible to analyze the polymer types and size of a large number of microplastic-like particles in less time. In this paper, we report a new semi-automated analysis device that combines reflectance-FTIR spectroscopy with imaging capabilities for rapid measurements of larger microplastics that can be recognized with the naked eye and handled with forceps. (Semi-) automated analytical technologies of microplastic that would significantly accelerate the otherwise labor-intensive and time-consuming process have been actively developed in recent years, particularly for small microplastics (<500 μm).[21–34] However, the development of (semi-) automated analytical technologies for larger microplastics has been relatively limited.[35–38]

Experimental methods

Microplastic analyzer using reflectance-FTIR semi-automatically (MARS)

We developed a semi-automated microplastic analysis system that combines a motorized stage, cameras for image acquisition, and FTIR for reflectance measurements (Fig. 1). This system allows for the final output of the number, size, and polymer type of microplastics placed on a sample plate into a Microsoft Excel file in a single procedure (Fig. S1†). The system, a Microplastic Analyzer using Reflectance-FTIR Semi-automatically (MARS), consists of an "imaging unit" that captures images to detect particles and measures their size (Fig. 1a), a "measurement unit" that measures the infrared reflectance of detected particles (Fig. 1b), and an "analysis unit" that determines the polymer types (Fig. 1c). In this system, only the process of placing the sample particles on a sample plate is performed manually, and all subsequent processes are

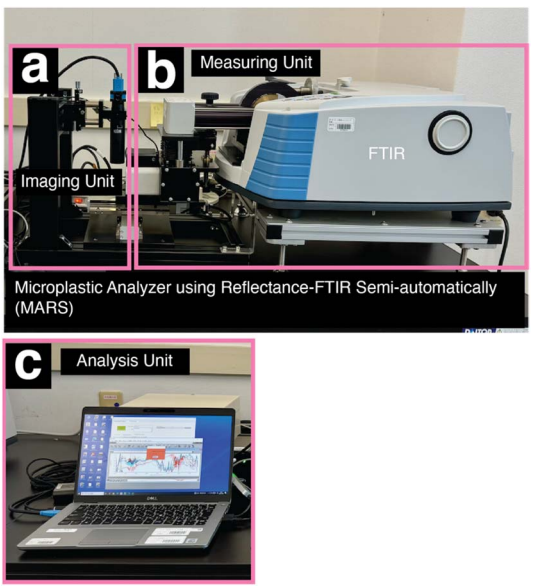

Fig. 1 Overview of the newly developed semi-automated analytical system of microplastics (Microplastic Analyzer using Reflectance-FTIR Semi-automatically, MARS). The system consists of (a) an imaging unit, (b) a measuring unit, and (c) an analysis unit. The details of each unit are described in Fig. 2–4.

© 2025 The Author(s). Published by the Royal Society of Chemistry

Open Access Article. Published on 10 February 2025. Downloaded on 5/28/2026 11:32:46 AM.
This article is licensed under a Creative Commons Attribution 3.0 Unported Licence.

completed automatically. Due to the inclusion of this manual step, we classify this device as a semi-automated system.

Imaging unit

Microplastic-like particles are manually placed on a sample plate. The sample plate is a rectangular mirror-polished stainless-steel SUS 304 plate measuring 70 mm × 50 mm (Fig. 2a and b). Particles can be randomly arranged on the sample plate without any restriction on the number of particles. However, particles must not overlap as overlapping particles will be recognized as a single particle as explained later. Additionally, particles must be at least 1 mm apart to ensure accurate infrared analysis; the reason for this will be explained later. The particles to be observed must be dry for FTIR analysis.

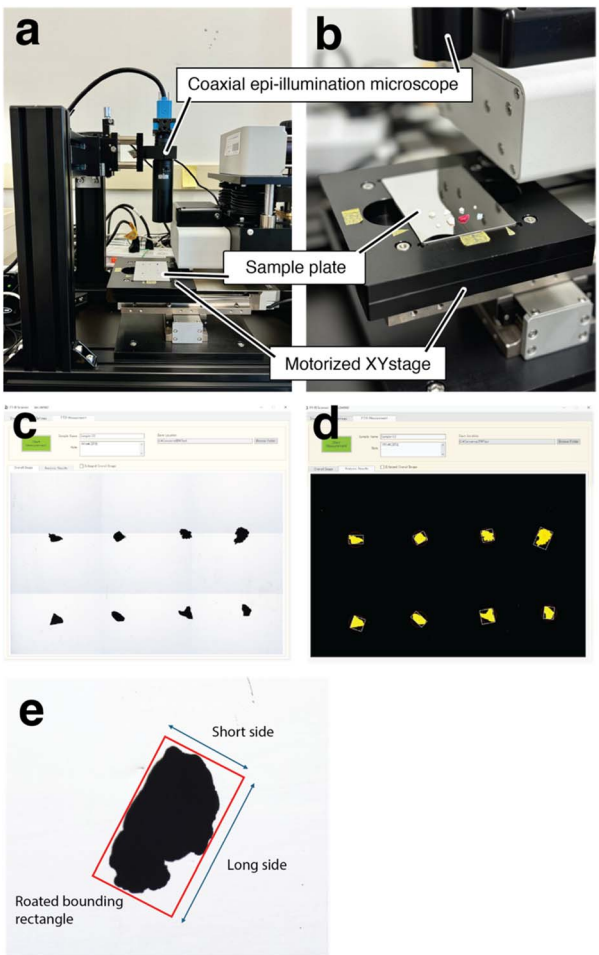

Fig. 2 Diagram of the imaging unit. (a) The imaging unit consists of a sample plate for placing the sample particles, a motorized *XY* stage, and a coaxial epi-illumination microscope camera. (b) The stainless-steel sample plate can hold as many sample particles as desired, as long as the conditions are met. The particles placed on the sample plate are captured by the coaxial epi-illumination microscope camera, and (c) after generating a composite image, (d) the particles on the sample plate are recognized. After capturing individual images of the recognized particles, (e) the long and short axes of the particles are provided based on the sides of the rotated bounding rectangle of the particles.

The sample plate with particles is placed on a motorized *XY* stage (Finesys Co., Ltd) (Fig. 2b). This motorized stage has space designed to fit the sample plate precisely. The stage can move 100 mm in both the *X* and *Y* directions, with a minimum movement of 0.001 mm and a repeat positioning accuracy of ±0.001 mm (Finesys Co., Ltd).

At the start of the measurement, the system recognizes particles on the sample plate (Fig. S1†). When the MARS system software, FT-IR scanner, is launched and "Start Measurement" is clicked, the sample plate is photographed using a coaxial epi-illumination microscope (MML06-HR65DV1-5M, Moritex Corp.) (Fig. 2a and b). The motorized stage moves the sample plate, allowing the microscope to capture images of the designated area of the sample plate. The area captured in one capture is 14 mm × 20 mm, so 15 images are required to capture the entire sample plate (3 horizontally and 5 vertically). The area to be captured on the sample plate can be changed arbitrarily. The multiple images are then automatically merged to create a single image of the designated area of the sample plate (Fig. 2c). Particles on the sample plate appear black in the images captured by the coaxial epi-illumination microscope camera, while the background appears white. Then, the images are converted to grayscale and subsequently binarized using Otsu's thresholding, allowing for particle recognition[39] (Fig. 2d). Then, the contours of particles are detected using the 'FindContours' function from OpenCV (an open-source image processing library) and detected particles are each assigned a number (Fig. 2d). After recognizing the coordinates of all the particles on the sample plate, each particle is individually photographed by the coaxial epi-illumination microscope. In order to measure the size of detected particles, the centroid position and coordinates of the corners (short and long sides) of each particle were obtained using 'BoxPoints' and 'MinAreaRect' from OpenCV. Here the long side and the short side refer to the sides of the rotated bounding rectangle of the particle (Fig. 2e). The size measurement includes (1) the short side and long side of each particle, (2) the aspect ratio of the long side to the short side, and (3) the area of the particle.

Measuring unit

After photographing and measuring the size of the particles in the imaging unit, the infrared spectra of each particle are obtained using reflectance FTIR (Fig. S1†). Based on the *XY* coordinate information of the particles, the motorized stage carrying the sample plate moves to position each particle directly beneath the infrared detector, allowing the acquisition of the infrared spectra by specular reflection.

The acquisition of infrared spectra was performed using a FTIR spectrometer with a liquid nitrogen-cooled mercury cadmium telluride (MCT) detector (Thermo Fisher Scientific, Nicolet iS10) (Fig. 3a). The wavelength range covered was 4500–650 cm^{-1}. We modified an external reflectance accessory (Thermo Fisher Scientific, ConservatIR) compatible with the sample compartment of the Nicolet iS10 for the analysis of microplastics (Fig. 3a and b). The extended reflection optics for FTIR, which illuminates and receives the reflected spectra, is

Open Access Article. Published on 10 February 2025. Downloaded on 5/28/2026 11:32:46 AM. This article is licensed under a Creative Commons Attribution 3.0 Unported Licence.

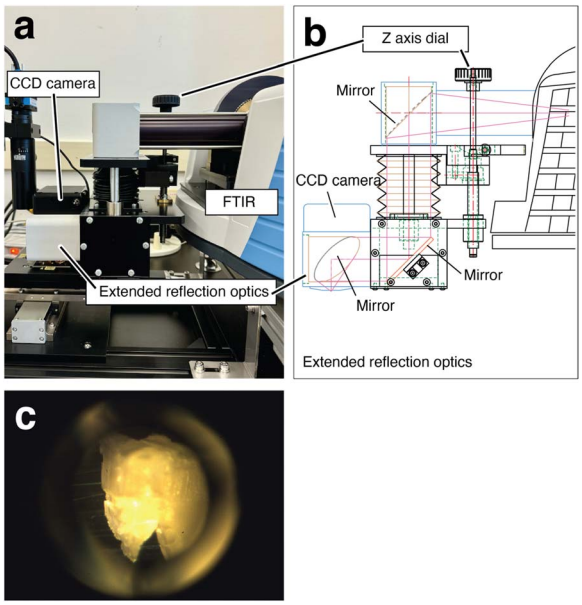

Fig. 3 Diagram of the measurement unit. (a) The analysis unit consists of the FTIR main body, an accessory for reflectance measurements of the sample particles that includes an extended reflection optics, a CCD camera integrated into the extended reflection optics, and a dial for adjusting focus along the *Z*-axis. (b) The reflectance measurement accessory is composed of three mirrors, with the mirror in the extended reflection optics being designed as a condenser, allowing infrared light to be concentrated on small particles for reflectance measurements. (c) A photograph of the microplastic particles captured by the CCD camera.

positioned directly beneath the sample plate using mirrors, enabling the measurement of particles on the plate (Fig. 3b). The extended reflection optics emits infrared light with a diameter of 1.25 mm through a mirror, and the reflected spectra from the sample and the underlying sample plate (a stainless-steel metal plate) are received by the detector.

A CCD camera integrated into the extended reflection optics provides a visible image of the illuminated area (Fig. 3b and c). An adjustment dial on the upper side of the extended reflection optics allows for the adjustment of the *Z*-axis, enabling the focusing of the particle image during measurement (Fig. 3b). The field of view of this CCD camera has a diameter of *ca.* 1 mm. In other words, to avoid capturing mixed spectra, only one particle or part of a particle should be within this 1 mm diameter range. Therefore, sample particles on the sample plate must be spaced at least 1 mm apart.

The acquisition of infrared spectra for the particles uses OMNIC, Thermo Fisher Scientific's analysis software, linked with the MARS system software, FTIR scanner. The number of scans can be adjusted in OMNIC, and 16 scans with a resolution of 4 cm^{-1} were performed in this study. Before performing FTIR measurements on the particles on the sample plate, a background measurement is automatically conducted. The background is obtained by measuring the infrared reflectance spectrum of a reference mirror mounted on the motorized *XY* stage.

Analysis unit

After obtaining the infrared spectra, the material identification is automatically initiated using Thermo Fisher Scientific's analysis software, OMNIC (Fig. S1†). The software can automatically search a designated folder containing the saved spectra and perform a library search of the obtained spectra to identify the polymer.

For the development of this analysis unit, a new library for the identification of degraded plastics was created specifically for reflectance measurements. Details of this library are described later. This degraded plastics identification library, combined with Thermo Fisher's conventional material library, is used to identify the materials of both plastic and non-plastic particles.

When the MARS system software is launched and the analysis starts, a folder with a user-defined name is created in a designated location (Fig. 4a) that consists of the generated data including the summary Excel file (Fig. 4b), microscope images for size measurement (Fig. 4c) and CCD camera images for FTIR measurement (Fig. 4d) of each particle, and spectral files (.SPA) of each measured particle (Fig. 4e). The measurement results of all particles on a single sample plate, including size and material identification results, are output to a single Excel file (Fig. 4b).

Development of a reference library for degraded plastic

We created a library of the representative spectra of different polymer types using OMNIC software (Thermo Fisher Scientific). To enable the identification of polymer types from the spectra of environmentally degraded plastics, we collected eight

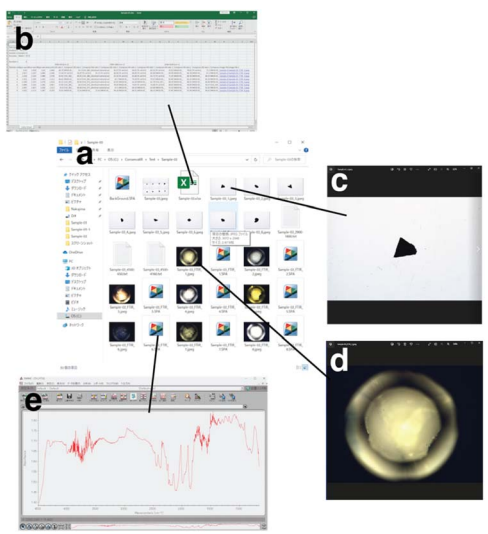

Fig. 4 Diagram of the analysis unit. After the analysis is completed by FTIR, the following information is saved in (a) a folder generated for each sample plate: (b) an Excel file containing the size of the measured particles and material identification results, (c) microscopic camera images of the measured particles, (d) CCD camera images for FTIR of the measured particles, (e) the spectra of the measured particles, and the blank spectra. (b) The generated Excel file displays the size of the measured particles (long axis, short axis, aspect ratio, and area) as well as the material identification results from the OMNIC library.

© 2025 The Author(s). Published by the Royal Society of Chemistry

Open Access Article. Published on 10 February 2025. Downloaded on 5/28/2026 11:32:46 AM. This article is licensed under a Creative Commons Attribution 3.0 Unported Licence.

polymer types of microplastics commonly observed in the marine environments.[40] The eight common plastics examined were: polyethylene (PE), polypropylene (PP), polystyrene (PS), polyvinyl chloride (PVC), polyethylene terephthalate (PET), polyamide (PA), ethylene-vinyl acetate (EVA), and polyurethane (PUR). These microplastics, excluding PVC and PUR, were sampled using surface-trawling neuston nets during surveys conducted in Sagami Bay, Japan, during several research cruises, as described in previous reports.[41,42] Other polymer types (PVC and PUR) were collected from the coastal environment near the outdoor premises of JAMSTEC.

The polymer types of all environmental microplastics were initially identified using an ATR-FTIR spectrometer (Thermo Fisher Scientific, Nicolet iS5). Samples were placed on the ATR crystal and compressed using the instrument clamp to ensure proper optical contact. During this process, minimal force was applied to avoid damaging the particles, and if significant damage occurred, the affected particles were excluded from subsequent reflectance measurements. Spectra were collected at a resolution of 4 cm^{-1} by averaging 16 scans per sample. Background measurements in air were taken every 60 minutes throughout the measurement process. Each obtained spectrum was then compared against several spectral database libraries, including both synthetic polymers and non-synthetic materials in OMNIC 9 software (Thermo Fisher Scientific). For subsequent analyses, 100 microplastic particles representing eight different polymer types (PE, PP, PS, PVC, EVA, PUR, PA, PET) were prepared.

Reflectance spectra for 100 particles each of the eight known polymer types were examined using the reflectance FTIR spectrometer. The spectral features of plastic particles from each polymer type were visually observed, and characteristics including (1) spectra with strong specular reflection (differentiated peak shape), (2) diffuse reflection spectra (low peak distortion, *i.e.*, absence of specular reflection), (3) spectra with a mix of specular and diffuse reflection, and (4) highly saturated spectra (where peak shapes are nearly unobservable) were visually identified (Fig. S2†). Finally, 100 spectra for each polymer type were visually classified into one of the aforementioned patterns. From each class, 2 to 3 representative spectra were randomly selected and averaged to generate a representative spectrum for that class. The spectra were smoothed using the Savitzky–Golay filter to reduce the impact of water vapor. Next, to determine whether the representative spectra of each class were suitable for identifying the types of polymers, we conducted discriminant analysis using TQ Analyst software (Thermo Fisher Scientific). Discriminant analysis evaluates samples by calculating the distance between the class center and the sample spectra. For discriminant analysis, the spectrum was normalized using the standard normal variate (SNV) to correct the vertical axis of the spectrum. The Mahalanobis distance was used to measure the distance from the center of each class to the spectra. The Mahalanobis distance indicates how well a sample matches a given class, and a smaller value signifies a higher likelihood that the sample belongs to that class. The distance to the next class represents the discriminant measure, with a higher distance ratio indicating a clearer discrimination.

Confirmation of the minimum size of analyzable microplastics

To determine the smallest microplastic size that MARS can reliably and automatically identify, we prepared environmentally collected PE particles of various sizes (approximately 100 μm, 200 μm, 300 μm, 400 μm, and 500 μm in diameter) and analyzed them using MARS. For each size category, 25 PE particles were prepared and analyzed using MARS. Averaged diameters of each size category were as follows: 107.6 ± 24.4 μm, 235.2 ± 38.3 μm, 314.2 ± 36.4 μm, 439.4 ± 63.4 μm, and 567.9 ± 76.4 μm, respectively. If more than 95% of the particles were correctly identified as PE, that size category was considered measurable by MARS.

Comparison with conventional methods

To evaluate how much time the newly developed semi-automated system (MARS) can save compared to conventional microplastic analysis methods, we compared MARS with traditional methods using ATR-FTIR, assuming the analysis of microplastics collected from the sea surface using nets. The comparison was conducted by two technicians, with one being an experienced technician with over five years of microplastic analysis experience and the other a novice technician who is analyzing microplastics for the first time. We prepared PE particles (200 particles) from the marine environments that had been collected by a neuston net as described earlier. The 200 PE microplastic particles were divided into eight sets of 25 particles each. Four sets were analyzed by the experienced technician, and the remaining four sets by the novice technician.

Initially, the time required for analysis using the conventional ATR-FTIR method was measured. The analysis included the following tasks: arranging sample particles, photographing and measuring sizes of particles, identifying materials with ATR-FTIR, and entering data into an Excel sheet. Each task's time was measured with a stopwatch. Arranging samples involved transferring the 25 microplastics to a numbered well plate with forceps. Photographing and measuring sizes involved capturing images of the microplastics on the well plate with a microscope (Olympus, SZX16) and a connected camera (Olympus, DP74) and measuring sizes with image analysis software (Olympus, cellSens Dimension 2.1). Material identification with ATR-FTIR involved measuring each microplastic one by one and determining their polymer types with the same setting described above. Finally, data entry involved recording the sizes and materials of the microplastics in an Excel sheet. After completing this series of tasks, the time required to measure the same 25 microplastics (four sets) using MARS was measured. This included placing the 25 microplastics on the MARS sample plate, clicking the start button, and obtaining size and material results output to an Excel sheet. The time required for the initial setup (*i.e.*, starting up the computer and optimizing the alignment) was not considered for both ATR-FTIR and MARS. The difference in microplastic analysis time between the conventional method and the MARS method was analyzed using a *t*-test. A *p*-value of 0.05 or less was considered statistically significant.

Open Access Article. Published on 10 February 2025. Downloaded on 5/28/2026 11:32:46 AM. This article is licensed under a Creative Commons Attribution 3.0 Unported Licence.

Results and discussion

Advantage in using reflectance-FTIR in analyzing larger microplastics

The reflection method in FTIR is commonly used in micro-FTIR for analyzing small microplastics on a filter,[43] but it is generally not used for larger microplastics that are visible to the naked eye and can be picked up with forceps. While it is technically feasible to use micro-FTIR to analyze such large microplastics,[43–45] several hundred micrometers in size, in such cases, each microplastic would need to be individually examined through a microscope while acquiring spectra by irradiating infrared light, a process that is more time-consuming than the ATR method. Moreover, a single large microplastic particle can extend beyond the microscope's field of view, making the analysis of large microplastics with micro-FTIR even more cumbersome. Additionally, the number of large microplastics that can be placed on the filter for analysis using micro-FTIR is limited due to the smaller filter diameter (*e.g.*, 25 mm) that can be scanned by micro-FTIR. The effort required to manually reposition large microplastics on a narrow filter area for each analysis further increases the operational time.[23] Furthermore, if large microplastics on the filter are to be imaged using a two-dimensional array, infrared information is acquired for all pixels within each large microplastic particle, which is simply a waste of time. Therefore, if large microplastics are to be analyzed, it is faster and more straightforward to use conventional, cost-effective ATR-FTIR without the need for the expensive micro-FTIR. Consequently, ATR-FTIR has been used for the analysis of large microplastics.

One of the issues with measuring microplastics using the ATR method is that the microplastics are often damaged because the sample is pressed against the prism during measurement.[13] After ATR measurement, the microplastics may crack or crumble into smaller pieces, making subsequent recovery difficult and limiting their further use (*e.g.*, for weight measurement). Therefore, in this study, to overcome the issues associated with ATR, a non-contact reflection method was employed for measuring large microplastics.

In conventional FTIR, the transmission method is also known as a non-contact technique. However, in the transmission method, it is necessary for the sample thickness to be less than approximately 10 μm to allow the infrared light to pass through.[8] Since it is not feasible to section microplastics, the transmission method is unsuitable for analyzing larger microplastic samples. Therefore, we consider that the use of the reflection method is suitable for the rapid and non-destructive measurement of large microplastics. Although a reflection measurement method using standard FTIR has existed, to the best of our knowledge, it had never been used for the analysis of larger microplastics. Although Thermo Fisher Scientific had developed an external reflection measurement accessory, ConservatIR, that could be attached to a conventional FTIR spectrometer, it was only capable of measuring objects positioned laterally (at 90° relative to gravity) or upwards (at 180° relative to gravity) from the FTIR. Therefore, we modified the reflection detector to face downward and enhanced it with a mirror to focus on and measure small objectives.

Development of a reflectance-FTIR spectral library, with plastic identities confirmed using ATR-FTIR

The ATR-FTIR and reflectance FTIR spectra of eight known environmentally degraded plastic polymers (PE, PP, PS, PET, PVC, PUR, EVA, PA) were compared (Fig. 5). As expected, the ATR-FTIR spectra showed relatively "simple" spectral profiles characterized by clear absorption bands on a uniform baseline, as has been previously reported.[20] The ATR-FTIR spectra depicted in Fig. 5 closely matched the spectral features reported in the literature,[46] and thus are superior for identifying polymers.

In contrast, the corresponding reflectance FTIR spectra displayed highly variable baselines due to distorted band shapes. These distortions are believed to be caused by the thickness and shape of the sample particles, which are thought to result in phenomena such as reflections from the sample surface (anomalous dispersion of the refractive index), absorption within the sample, and diffuse reflection.[20]

Despite these limitations, the reflectance FTIR spectra still contained the necessary chemical information for polymer identification. The comparison of reflectance and ATR-FTIR spectra identified the general regions of interest for polymer absorption bands, including the CH stretching region (3000–

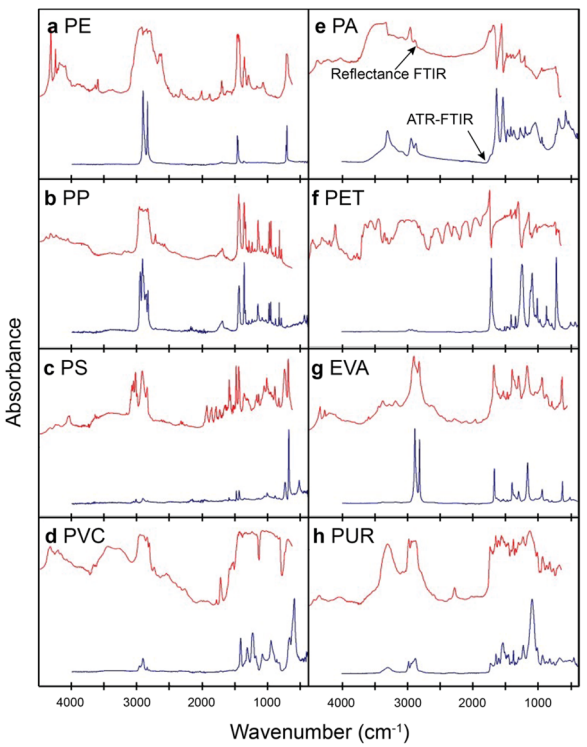

Fig. 5 Comparison of ATR-FITR (bottom track, blue) and reflectance FTIR spectra (top trace, red) with MARS for eight different polymer types of microplastics collected from the environment: (a) polyethylene (PE), (b) polypropylene (PP), (c) polystyrene (PS), (d) polyvinyl chloride (PVC), (e) polyethylene terephthalate (PET), (f) polyamide (PA), (g) ethylene-vinyl acetate (EVA), and (h) polyurethane (PUR).

© 2025 The Author(s). Published by the Royal Society of Chemistry

Open Access Article. Published on 10 February 2025. Downloaded on 5/28/2026 11:32:46 AM. This article is licensed under a Creative Commons Attribution 3.0 Unported Licence.

Table 1 Discriminant analysis results of different polymer types based on reflectance-FTIR spectra. PE, polyethylene; PP, polypropylene; PS, polystyrene; PVC, polyvinyl chloride; PET, polyethylene terephthalate; PA, polyamide; EVA, ethylene-vinyl acetate; PUR, polyurethane

Actual class	Calculated class	Distance	Next class	Next distance	Mahalanobis ratio
PE-1	PE	1.0	EVA	1.78	1.7
PE-2	PE	0.4	EVA	2.33	5.9
PE-3	PE	0.5	EVA	2.1	4.7
PE-4	PE	0.6	EVA	2.1	3.4
EVA-1	EVA	0.5	PE	1.8	3.6
EVA-2	EVA	1.0	PE	2.3	2.3
EVA-3	EVA	1.0	PA	2.4	2.4
EVA-4	EVA	0.7	PE	1.4	1.9
PP-1	PP	0.6	PVC	3.6	5.6
PP-2	PP	0.8	PVC	3.3	4.4
PP-3	PP	1.0	PVC	3.7	3.6
PP-4	PP	1.0	PVC	4.1	4.1
PVC-1	PVC	0.9	EVA	3.2	3.4
PVC-2	PVC	1.0	EVA	3.9	3.8
PVC-3	PVC	1.0	EVA	4.1	4.3
PUR-1	PUR	0.9	PS	3.5	3.9
PUR-2	PUR	0.9	PS	3.3	3.7
PA-1	PA	1.0	EVA	3.5	3.4
PA-2	PA	1.0	EVA	2.7	2.7
PA-3	PA	1.0	EVA	3.2	3.2
PS-1	PS	0.1	PUR	3.2	36.0
PS-2	PS	0.1	PUR	3.3	36.3
PET-1	PET	0.6	PP	4.2	7.1
PET-2	PET	0.6	PS	4.2	7.2

2800 cm^{-1}), the CH bending region (1470–1365 cm^{-1}), the carbonyl stretching region (1820–1680 cm^{-1}), and the NH stretching region of PA (3500–3300 cm^{-1}).[20,46] Particularly, the range in the near-infrared region around 4400–4100 cm^{-1}, which includes a combination of CH stretching and CH bending vibration and where spectral saturation and specular reflection are minimal, resulted in the large Mahalanobis distance ratio between the designated class and the nearest class (Table 1).

The results of the discriminant analysis indicated that all eight polymer types were classified into their respective classes (Table 1). The distances were relatively large, demonstrating the ability to distinguish specific types of polymers. The number of target spectra and the number of successfully identified spectra for each type of polymer are listed in Table 2. The results of the library search indicated that more than 98% of the spectra were recognized as the same polymer types identified with ATR-FTIR. These findings suggest that, although the reflectance FTIR spectra may appear complex, they are capable of extracting sufficient chemical information to enable the identification of polymers even in degraded plastics collected from the environment, using multivariate statistics.

Table 2 Results of the library search using TQ Analyst software based on the discriminant analysis

Polymer type	Number of target spectra	Success rate (%)
PE	100	97
PP	100	97
PS	100	98
PET	100	100
PVC	100	95
PUR	100	100
EVA	100	100
PA	100	100
Overall	98.4 ± 1.9	

The minimum size detectable by MARS

The results of measuring 25 PE particles with diameters of approximately 100, 200, 300, 400 and 500 μm using MARS showed that the smaller the particle size, the lower the accuracy of identification as PE. In this test, the accuracy of material identification was 0% for 100 μm particles and 16% for 200 μm particles. For larger sizes, the accuracy improved significantly, reaching 76% for 300 μm particles and 100% for both 400 μm and 500 μm particles (Table 3). Therefore, the minimum particle size that can be reliably and automatically identified using the MARS system was approximately 400 μm.

The decrease in accuracy for smaller particles may be attributed to multiple factors related to the physical properties of the particles and the limitations of the MARS detection system. As particle size decreases, the surface area-to-volume ratio increases, which amplifies the effects of surface phenomena such as distortion and diffuse reflection. Smaller particles, due to their increased curvature and surface irregularities, tend to scatter light more diffusely. This diffuse scattering reduces the intensity of the reflected spectral data and alters its path, potentially making it difficult for the detector to capture sufficient and accurate signals required for material identification. It is also possible that, for particles <400 μm, spectral information from optical systems other than the resin is being reflected, which may lead to a decrease in library search accuracy. To address these challenges, further technological advancements in the MARS system should be considered. For instance, the use of a Cassegrain mirror to focus infrared light specifically on the target area at high magnification could enhance detector sensitivity. Such improvements could play a pivotal role in improving the system's ability to accurately identify smaller particles.

Comparison with conventional methods

The time required for conventional analytical methods, including ATR-FTIR, to analyze 25 microplastic particles, from numbering the sample particles to entering their size and material into an Excel sheet, was 108.2 ± 5.2 (mean ± standard deviation) min for an experienced technician and 194.2 ± 14.4 min for a novice technician (overall mean: 151.2 ± 45.0 min) (Fig. 6). In contrast, the time required to measure the same 25 sample particles using MARS was significantly shorter than with conventional methods: 22.4 ± 2.2 min for the experienced technician (4.8 times faster) and 23.7 ± 1.0 minutes for the novice technician (8.2 times faster), with an overall mean of 23.0 ± 1.7 min ($p < 0.0001$ for all conditions). Overall, MARS was 6.6 times faster than conventional methods.

Open Access Article. Published on 10 February 2025. Downloaded on 5/28/2026 11:32:46 AM.
This article is licensed under a Creative Commons Attribution 3.0 Unported Licence.

Table 3 Results of the test for the minimum size of analyzable microplastics using MARS. PE: polyethene. The diameter of each particle is the average of its long axis and short axis

	100 μm		200 μm		300 μm		400 μm		500 μm	
Particle no.	Diameter (μm)	Identified material	Diameter (μm)	Identified material	Diameter (μm)	Identified material	Diameter (μm)	Identified material	Diameter (μm)	Identified material
1	94.5	Acrylic resin	250	Acrylic resin	303	PE	375.5	PE	498	PE
2	103.5	Acrylic resin	241	Acrylic resin	385	PE	399.5	PE	480	PE
3	97	Acrylic resin	264	Acrylic resin	331	Acrylic resin	382	PE	566.5	PE
4	117.5	Acrylic resin	180	Acrylic resin	264	Acrylic resin	398	PE	505	PE
5	96.5	Acrylic resin	193.5	Acrylic resin	305.5	PE	466	PE	478.5	PE
6	101.5	Acrylic resin	211	Acrylic resin	305.5	Acrylic resin	395.5	PE	636.5	PE
7	138.5	Acrylic resin	197.5	Acrylic resin	357.5	PE	459	PE	597	PE
8	83	Acrylic resin	236.5	Acrylic resin	347.5	PE	424.5	PE	513	PE
9	93.5	Acrylic resin	201.5	Acrylic resin	271.5	PE	408.5	PE	687	PE
10	120.5	Acrylic resin	219	Acrylic resin	283	PE	405	PE	588	PE
11	174.5	Acrylic resin	218	PE	304	PE	363	PE	579	PE
12	113	Acrylic resin	211.5	Acrylic resin	332	PE	426.5	PE	461	PE
13	100	Acrylic resin	248	Acrylic resin	255	Acrylic resin	439	PE	579.5	PE
14	109.5	Acrylic resin	208	Acrylic resin	310.5	PE	500.5	PE	579	PE
15	106	Acrylic resin	248.5	Acrylic resin	315	PE	400.5	PE	639	PE
16	88	Acrylic resin	264	Acrylic resin	298	PE	404	PE	497	PE
17	111	Acrylic resin	221.5	Acrylic resin	307.5	PE	531	PE	543.5	PE
18	98	Acrylic resin	271.5	PE	287.5	Acrylic resin	444	PE	540	PE
19	122.5	Acrylic resin	208	Acrylic resin	333.5	PE	424.5	PE	560.5	PE
20	82	Acrylic resin	280	PE	319	PE	367	PE	670.5	PE
21	82	Acrylic resin	246.5	Acrylic resin	266.5	PE	514	PE	482	PE
22	103.5	Acrylic resin	247	Acrylic resin	295.5	Acrylic resin	467.5	PE	694	PE
23	139.5	Acrylic resin	336	PE	380.5	PE	498	PE	558.5	PE
24	128	Acrylic resin	303	Acrylic resin	308	PE	650	PE	748	PE
25	86	Acrylic resin	173.5	Acrylic resin	388	PE	443	PE	516	PE
	107.6 ± 21.4	0%	235.2 ± 38.3	16%	314.2 ± 36.4	76%	439.4 ± 63.4	100%	567.9 ± 76.4	100%

© 2025 The Author(s). Published by the Royal Society of Chemistry

Open Access Article. Published on 10 February 2025. Downloaded on 5/28/2026 11:32:46 AM. This article is licensed under a Creative Commons Attribution 3.0 Unported Licence.

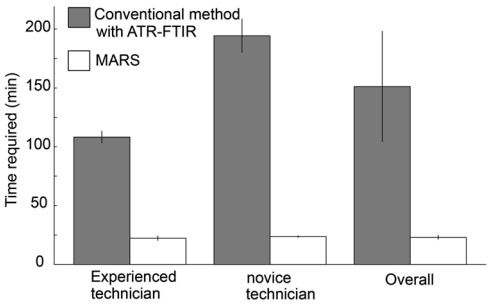

Fig. 6 Comparison of analysis time (min) for measuring 25 microplastic particles using conventional methods with ATR-FTIR and MARS for experienced and novice technicians. Error bars indicate standard deviation of the mean values. The analysis time includes sample particle placement, microscopic imaging, size data acquisition, FTIR analysis, and entry of results into an Excel file.

Even for the experienced technician, analyzing 25 particles using the conventional method took 108 min, meaning that analyzing 1000 particles would take 72 h—a task that would require nine days at eight hours of work per day. In contrast, using MARS, analyzing 1000 particles would take only 14.9 h. Although it is currently physically impossible to place 1000 particles on a single sample plate, even if the sample is divided and measured multiple times, the task could still be completed within two 8 hours workdays. This substantial reduction in microplastic analysis time suggests that the utilization of MARS will enable the analysis of larger quantities of samples within a limited timeframe.

Furthermore, while the experienced technician completed the analysis significantly faster than the novice technician using conventional methods ($p < 0.0001$), no significant difference was observed between experienced and novice technicians when using MARS ($p = 0.310$). This indicates that, unlike conventional methods where experienced technicians are naturally faster, MARS requires minimal manual intervention beyond placing the sample particles on the sample plate. Once the particles are on the plate, the system automatically determines the size and material, and then outputs an Excel sheet that summarizes the data, eliminating the speed differential due to technician experience. This means that anyone, regardless of their level of experience, can obtain results at the same speed using MARS.

In conventional ATR-FTIR methods, the standard approach is to analyze all particles that resemble microplastics. However, there is a possibility that microplastic particles that do not visually appear as microplastics may have been overlooked, which may introduce investigator bias. In contrast, MARS allows for the simultaneous placement and analysis of both microplastic-like particles and visually non-microplastic particles on the sample plate and completes the analysis within a short time. Therefore, investigator bias is expected to be reduced compared to conventional methods.

Limitations

The MARS system is currently incapable of accurately identifying microplastics smaller than 400 μm. Large microplastics (500 μm–5 mm) that can be easily recognized with the naked eye and reliably handled with forceps, as defined in many studies,[10,14] can be effectively analyzed automatically with MARS. However, given that the mesh size of standard manta nets and neuston nets for microplastic sampling is approximately 300 μm,[47] MARS cannot comprehensively analyze all particles collected by these nets. Particles smaller than 400 μm must still be analyzed using conventional methods such as the ATR-FTIR method, as has been the standard practice. Advancements in the MARS detection system, such as the introduction of a Cassegrain mirror as described above, are expected to enhance the system to analyze a larger proportion of microplastics collected by net sampling in the future. This improvement would greatly enhance the capability of MARS to handle a broader range of particle size.

Additionally, the current model of MARS relies on a relatively small spectral library encompassing only eight polymer types, which limits its accuracy in identifying less common polymers or emerging synthetic materials. To enable broader applications and improve its utility, continuous updates and expansion of the spectral library will be essential. These developments will ensure the system remains adaptable to the growing diversity of polymers encountered in environmental samples.

Conclusion

In conclusion, MARS represents a significant step forward in the semi-automated analysis of large microplastics, offering a substantial reduction in analysis time and requiring minimal technician experience to operate. The system's integration of reflectance-FTIR spectroscopy, image recognition, and motorized stage automation has demonstrated remarkable improvements in the efficiency of microplastic quantification and polymer identification, with accuracy rates exceeding 98% for large particles. Despite limitations, such as the inability to accurately detect smaller microplastics (<400 μm) and certain complexities in spectral interpretation, MARS holds great potential for accelerating global microplastic research and monitoring. Its ability to streamline the processing of large microplastic samples can significantly enhance the understanding of microplastic distribution in aquatic environments, making it a valuable tool for environmental scientists and policymakers alike. Future improvements, including enhanced spectral libraries, will further extend its applicability and reliability.

Data availability

The data supporting this article have been included as part of the ESI.†

Author contributions

Ryota Nakajima: conceptualization, methodology, writing – original draft, visualization, funding acquisition. Hiromi Sawada, Shinichiro Hayashi, Akishi Nara: methodology, visualization, writing – review & editing. Mitsunari Hattori:

Open Access Article. Published on 10 February 2025. Downloaded on 5/28/2026 11:32:46 AM. This article is licensed under a Creative Commons Attribution 3.0 Unported Licence.

conceptualization, methodology, visualization, funding acquisition, writing – review & editing.

Conflicts of interest

M. Hattori, H. Sawada, S. Hayashi, and A. Nara are employees of Thermo Fisher Scientific, the company that developed and marketed the FTIR used in the automated microplastic analysis system developed in this study.

Acknowledgements

The authors thank Y. Ueno, R. Matsui, and T. Morotomi for their help in testing the developed instrument, and N. Akeboshi (Finesys) for his contribution in developing the software. This study was funded by JAMSTEC to RN and Thermo Fisher Scientific to HS, SH, AN and MH.

References

1 N. Ali, M. H. Khan, M. Ali, S. Ahmad, A. Khan, G. Nabi, F. Ali, M. Bououdina and G. Z. Kyzas, Insight into microplastics in the aquatic ecosystem: Properties, sources, threats and mitigation strategies, *Sci. Total Environ.*, 2023, 169489.
2 K. L. Law and R. C. Thompson, Microplastics in the seas, *Science*, 2014, **345**, 144–145.
3 A. Ashrafy, A. A. Liza, M. N. Islam, M. M. Billah, S. T. Arafat, M. M. Rahman and S. M. Rahman, Microplastics pollution: a brief review of its source and abundance in different aquatic ecosystems, *J. Hazard. Mater. Adv.*, 2023, **9**, 100215.
4 M. Khoshmanesh, A. M. Sanati and B. Ramavandi, Co-occurrence of microplastics and organic/inorganic contaminants in organisms living in aquatic ecosystems: A review, *Mar. Pollut. Bull.*, 2023, **187**, 114563.
5 U. N. E. Programme, *Turning off the Tap. How the World Can End Plastic Pollution and Create a Circular Economy*, Nairobi, 2023.
6 J. Brandt, F. Fischer, E. Kanaki, K. Enders, M. Labrenz and D. Fischer, Assessment of subsampling strategies in microspectroscopy of environmental microplastic samples, *Front. Environ. Sci.*, 2021, **8**, 579676.
7 P. J. Kershaw, *Sources, Fate and Effects of Microplastics in the Marine Environment: A Global Assessment*, 2015.
8 A. Käppler, M. Fischer, B. M. Scholz-Böttcher, S. Oberbeckmann, M. Labrenz, D. Fischer, K.-J. Eichhorn and B. Voit, Comparison of μ-ATR-FTIR spectroscopy and py-GCMS as identification tools for microplastic particles and fibers isolated from river sediments, *Anal. Bioanal. Chem.*, 2018, **410**, 5313–5327.
9 K. Munno, H. De Frond, B. O'Donnell and C. M. Rochman, Increasing the accessibility for characterizing microplastics: introducing new application-based and spectral libraries of plastic particles (SLoPP and SLoPP-E), *Anal. Chem.*, 2020, **92**, 2443–2451.
10 V. Hidalgo-Ruz, L. Gutow, R. C. Thompson and M. Thiel, Microplastics in the marine environment: a review of the methods used for identification and quantification, *Environ. Sci. Technol.*, 2012, **46**, 3060–3075.
11 M. Zobkov and E. Esiukova, Microplastics in a Marine Environment: Review of Methods for Sampling, Processing, and Analyzing Microplastics in Water, Bottom Sediments, and Coastal Deposits, *Oceanology*, 2018, **58**, 137–143.
12 A. Isobe, N. T. Buenaventura, S. Chastain, S. Chavanich, A. Cózar, M. DeLorenzo, P. Hagmann, H. Hinata, N. Kozlovskii and A. L. Lusher, An interlaboratory comparison exercise for the determination of microplastics in standard sample bottles, *Mar. Pollut. Bull.*, 2019, **146**, 831–837.
13 W. J. Shim, S. H. Hong and S. E. Eo, Identification methods in microplastic analysis: a review, *Anal. Methods*, 2017, **9**, 1384–1391.
14 M. G. Löder and G. Gerdts, Methodology used for the detection and identification of microplastics—a critical appraisal, *Marine Anthropogenic Litter*, 2015, pp. 201–227.
15 G. Renner, T. C. Schmidt and J. R. Schram, A new chemometric approach for automatic identification of microplastics from environmental compartments based on FT-IR spectroscopy, *Anal. Chem.*, 2017, **89**, 12045–12053.
16 L. Mai, L.-J. Bao, L. Shi, C. S. Wong and E. Y. Zeng, A review of methods for measuring microplastics in aquatic environments, *Environ. Sci. Pollut. Res.*, 2018, **25**, 11319–11332.
17 J. N. Möller, M. G. Löder and C. Laforsch, Finding microplastics in soils: a review of analytical methods, *Environ. Sci. Technol.*, 2020, **54**, 2078–2090.
18 Z. Huang, B. Hu and H. Wang, Analytical methods for microplastics in the environment: a review, *Environ. Chem. Lett.*, 2023, **21**, 383–401.
19 J. C. Prata, J. P. Da Costa, A. C. Duarte and T. Rocha-Santos, Methods for sampling and detection of microplastics in water and sediment: A critical review, *TrAC, Trends Anal. Chem.*, 2019, **110**, 150–159.
20 M. Willans, E. Szczecinski, C. Roocke, S. Williams, S. Timalsina, J. Vongsvivut, J. McIlwain, G. Naderi, K. L. Linge and M. J. Hackett, Development of a rapid detection protocol for microplastics using reflectance-FTIR spectroscopic imaging and multivariate classification, *Environ. Sci.: Adv.*, 2023, **2**, 663–674.
21 Z. Yang, M. Çelik and H. Arakawa, Challenges of Raman spectra to estimate carbonyl index of microplastics: a case study with environmental samples from sea surface, *Mar. Pollut. Bull.*, 2023, **194**, 115362.
22 Q. T. Whiting, K. F. O'Connor, P. M. Potter and S. R. Al-Abed, A high-throughput, automated technique for microplastics detection, quantification, and characterization in surface waters using laser direct infrared spectroscopy, *Anal. Bioanal. Chem.*, 2022, **414**, 8353–8364.
23 Y. K. Song, S. H. Hong, S. Eo and W. J. Shim, A comparison of spectroscopic analysis methods for microplastics: manual, semi-automated, and automated Fourier transform infrared and Raman techniques, *Mar. Pollut. Bull.*, 2021, **173**, 113101.

© 2025 The Author(s). Published by the Royal Society of Chemistry

Open Access Article. Published on 10 February 2025. Downloaded on 5/28/2026 11:32:46 AM. This article is licensed under a Creative Commons Attribution 3.0 Unported Licence.

24 G. Renner, T. C. Schmidt and J. Schram, Automated rapid & intelligent microplastics mapping by FTIR microscopy: A Python–based workflow, *MethodsX*, 2020, **7**, 100742.
25 J. Rausch, D. Jaramillo-Vogel, S. Perseguers, N. Schnidrig, B. Grobéty and P. Yajan, Automated identification and quantification of tire wear particles (TWP) in airborne dust: SEM/EDX single particle analysis coupled to a machine learning classifier, *Sci. Total Environ.*, 2022, **803**, 149832.
26 S. Primpke, C. Lorenz, R. Rascher-Friesenhausen and G. Gerdts, An automated approach for microplastics analysis using focal plane array (FPA) FTIR microscopy and image analysis, *Anal. Methods*, 2017, **9**, 1499–1511.
27 J. C. Prata, V. Reis, J. T. Matos, J. P. da Costa, A. C. Duarte and T. Rocha-Santos, A new approach for routine quantification of microplastics using Nile Red and automated software (MP-VAT), *Sci. Total Environ.*, 2019, **690**, 1277–1283.
28 C.-G. Pan, S. M. Mintenig, P. E. Redondo-Hasselerharm, P. H. Neijenhuis, K.-F. Yu, Y.-H. Wang and A. A. Koelmans, Automated μFTIR imaging demonstrates taxon-specific and selective uptake of microplastic by freshwater invertebrates, *Environ. Sci. Technol.*, 2021, **55**, 9916–9925.
29 S. R. Moses, L. Roscher, S. Primpke, B. Hufnagl, M. G. Löder, G. Gerdts and C. Laforsch, Comparison of two rapid automated analysis tools for large FTIR microplastic datasets, *Anal. Bioanal. Chem.*, 2023, **415**, 2975–2987.
30 W. Jia, A. Karapetrova, M. Zhang, L. Xu, K. Li, M. Huang, J. Wang and Y. Huang, Automated identification and quantification of invisible microplastics in agricultural soils, *Sci. Total Environ.*, 2022, **844**, 156853.
31 E. Von Der Esch, A. J. Kohles, P. M. Anger, R. Hoppe, R. Niessner, M. Elsner and N. P. Ivleva, TUM-ParticleTyper: A detection and quantification tool for automated analysis of (Microplastic) particles and fibers, *PLoS One*, 2020, **15**, e0234766.
32 M. Dong, Z. She, X. Xiong, G. Ouyang and Z. Luo, Automated analysis of microplastics based on vibrational spectroscopy: are we measuring the same metrics?, *Anal. Bioanal. Chem.*, 2022, **414**, 3359–3372.
33 E. Nicolai, R. Pizzoferrato, Y. Li, S. Frattegiani, A. Nucara and G. Costa, A new optical method for quantitative detection of microplastics in water based on real-time fluorescence analysis, *Water*, 2022, **14**, 3235.
34 D. Calore and N. Fraticelli, State of the art offshore in situ monitoring of microplastic, *Microplastics*, 2022, **1**, 640–650.
35 N. Meyers, A. I. Catarino, A. M. Declercq, A. Brenan, L. Devriese, M. Vandegehuchte, B. De Witte, C. Janssen and G. Everaert, Microplastic detection and identification by Nile red staining: Towards a semi-automated, cost-and time-effective technique, *Sci. Total Environ.*, 2022, **823**, 153441.
36 X.-L. Han, N.-J. Jiang, T. Hata, J. Choi, Y.-J. Du and Y.-J. Wang, Deep learning based approach for automated characterization of large marine microplastic particles, *Mar. Environ. Res.*, 2023, **183**, 105829.
37 L. Frère, I. Paul-Pont, J. Moreau, P. Soudant, C. Lambert, A. Huvet and E. Rinnert, A semi-automated Raman micro-spectroscopy method for morphological and chemical characterizations of microplastic litter, *Mar. Pollut. Bull.*, 2016, **113**, 461–468.
38 A. J. Beck, M. Kaandorp, T. Hamm, B. Bogner, E. Kossel, M. Lenz, M. Haeckel and E. P. Achterberg, Rapid shipboard measurement of net-collected marine microplastic polymer types using near-infrared hyperspectral imaging, *Anal. Bioanal. Chem.*, 2023, **415**, 2989–2998.
39 K. Saddami, K. Munadi, Y. Away and F. Arnia, Improvement of binarization performance using local otsu thresholding, *Int. J. Electr. Comput. Eng.*, 2019, **9**, 1–8.
40 R. Geyer, J. R. Jambeck and K. L. Law, Production, use, and fate of all plastics ever made, *Sci. Adv.*, 2017, **3**, e1700782.
41 R. Nakajima, T. Miyama, T. Kitahashi, N. Isobe, Y. Nagano, T. Ikuta, K. Oguri, M. Tsuchiya, T. Yoshida, K. Aoki, Y. Maeda, K. Kawamura, M. Suzukawa, T. Yamauchi, H. Ritchie, K. Fujikura and A. Yabuki, Plastic after an extreme storm: The typhoon-induced response of micro-and mesoplastics in coastal waters, *Front. Mar. Sci.*, 2022, **8**, 806952.
42 R. Nakajima, A. Nagano, S. Osafune, M. Tsuchiya and K. Fujikura, Aggregation and transport of microplastics by a cold-core ring in the southern recirculation of the Kuroshio Extension: the role of mesoscale eddies on plastic debris distribution, *Ocean Dyn.*, 2024, **74**, 773–782.
43 C. Rathore, M. Saha, P. Gupta, M. Kumar, A. Naik and J. de Boer, Standardization of micro-FTIR methods and applicability for the detection and identification of microplastics in environmental matrices, *Sci. Total Environ.*, 2023, **888**, 164157.
44 X. Meng, T. Bao, L. Hong and K. Wu, Occurrence characterization and contamination risk evaluation of microplastics in Hefei's urban wastewater treatment plant, *Water*, 2023, **15**, 686.
45 Y. K. Song, S. H. Hong, M. Jang, G. M. Han, M. Rani, J. Lee and W. J. Shim, A comparison of microscopic and spectroscopic identification methods for analysis of microplastics in environmental samples, *Mar. Pollut. Bull.*, 2015, **93**, 202–209.
46 M. R. Jung, F. D. Horgen, S. V. Orski, V. Rodriguez, K. L. Beers, G. H. Balazs, T. T. Jones, T. M. Work, K. C. Brignac and S.-J. Royer, Validation of ATR FT-IR to identify polymers of plastic marine debris, including those ingested by marine organisms, *Mar. Pollut. Bull.*, 2018, **127**, 704–716.
47 Y. Michida, S. Chavanich, S. Chiba, M. R. Cordova, A. Cozsar Cabanas, F. Glagani, P. Hagmann, H. Hinata, A. Isobe and P. Kershaw, Guidelines for Harmonizing Ocean Surface Microplastic Monitoring Methods, Version 1.1, 2019.